



Stiffness of Ballastless Railway Embankments Determined by Repetitive Static Plate Load Tests

Carl Wersäll¹ · Sadek Baker² · Peter Zackrisson³

Accepted: 4 July 2022 / Published online: 27 July 2022
© The Author(s) 2022

Abstract

In the repetitive static plate load test, a plate is loaded in two cycles where the second loading cycle provides a modulus denoted E_{v2} . When calculating the stiffness of a railway embankment, Young's modulus is often assumed to be equal to E_{v2} throughout the embankment. This approach, however, provides inaccurate results, mainly due to soil nonlinearity and the influence of confinement stress. Currently, there exists no method to account for these aspects to derive reliable deformation properties of embankments. Occasionally, correction factors are applied to E_{v2} , resulting in crude estimations. In this study, plate load tests were simulated in PLAXIS 2D using the Hardening Soil Model and calibrated against four field tests, conducted on crushed rock-fill sub-ballast. The calibrated soil properties were applied in finite element simulations of railway embankments with ballastless slab-track systems. Based on the results of finite element analyses, a semi-empirical approach is proposed, which considers confinement stress through a hyperbolic stress–strain relationship. Soil properties for compacted rock-fill with particle grading 0–150 mm were assumed through the results of the calibrated finite element analyses and the method was verified against 43 plate load tests. This semi-empirical method is more accurate than assuming a constant Young's modulus, while maintaining simplicity and ease of use.

Keywords Plate load test · E_{v2} · High-speed railway embankment · Slab track

✉ Carl Wersäll
cwersall@kth.se

Sadek Baker
sadek.baker@kerberosgeo.se

Peter Zackrisson
peter.zackrisson@trafikverket.se

¹ KTH Royal Institute of Technology, Department of Civil and Architectural Engineering, Brinellvägen 23, 100 44 Stockholm, Sweden

² Kerberos Geoteknik, Riddargatan 17, 114 57 Stockholm, Sweden

³ The Swedish Transport Administration, Röda vägen 1, 781 70, Borlänge, Sweden

1 Introduction

Vertical embankment stiffness is often determined in the field by the static plate load test (PLT), shown in Fig. 1. In Europe, the repetitive static PLT, in which the plate is loaded in two cycles, is common. Execution of the PLT is standardized and regulated in various national standards. The evaluation method varies slightly in different standards. In this study, evaluation is conducted according to German and Swedish standards (Deutsches Institut für Normung 2012; Trafikverket 2014). Different diameters of loading plates are allowed, but the most common is 300 mm. For the 300-mm diameter plate, the load is applied in stages up to 500 kPa in the first cycle, after which unloading is conducted in stages until the stress is zero, followed by the second stage-wise loading cycle until 450 kPa. Maximum loads are different for other plate diameters. Plate settlement is measured during the loading process. Vertical loading moduli are obtained for the first and second cycles of the stress-settlement measurements by fitting second-degree polynomials via the least square method and calculating the modulus from 30 to 70% of the maximum load. The moduli for the first and second cycles are denoted E_{v1} and E_{v2} , respectively. The evaluation assumes that Poisson's ratio is 0.21.

The E_{v2} modulus is considered to be the most representative of embankment stiffness and is used mainly as a requirement for compaction control. However, it is not an accurate representation of Young's modulus (E) that governs operational deformations of embankments and should therefore not be used directly in embankment design (Elsamee 2013; Dastich and Dawson 1995; Kim and Park 2011; Gomes Correia et al. 2004a; Gomes Correia and Cunha 2014). The main reasons for the unsuitability in representing embankment stiffness by E_{v2} can be summarized as follows:

1. Loading area. The loading plate is circular and typically 300 mm in diameter. If the loading area in the operational stage is larger, such as a distributed load (e.g., a soil layer) or a slab (e.g., a ballastless railway track), the load reaches a greater

Fig. 1 Static PLT with 300-mm diameter plate and a truck as counterweight



soil depth where stiffness is higher due to higher overburden pressure, which affects the loading response.

2. Stress magnitude. The static PLT is conducted up to a contact stress of 500 kPa in the first loading cycle and 450 kPa in the second loading cycle (for a 300-mm diameter plate). The applied stress during operation is often significantly lower. Due to nonlinear deformation properties of the soil material, the stress magnitude has a great influence on the deformation behavior and thus on the Young's modulus. The E_{v2} -modulus is therefore only representative for the secant modulus at a stress magnitude of 450 kPa.

Currently, there exists no practical method to account for stress- and strain-dependent properties in evaluation of PLTs, to the best of the authors' knowledge. The effect of the aspects listed above is especially relevant for ballastless (slab track) railway systems, where the area loaded by the slab is several meters wide and the cyclic stress below the slab is a fraction of the stress applied during PLT. The depth below the load that has most significant influence on the response is typically estimated to be around two times the diameter of the load (in the case of a circular loading area) (Burmister 1947; Ping and Ge 1997). Gomes Correia et al. (Gomes Correia et al. 2004b) found in nonlinear simulations that 90% of settlements occur within a depth of two times the plate diameter. Since stiffness increases with stress and thus depth, a larger loading area will experience a stiffer soil response. Elsamee (Elsamee 2013) conducted loading tests on compacted sand with loading plates of various sizes and found that a larger plate yielded a greater settlement modulus. In addition, soil close to the surface may be loosened due to roller compaction (Gomes Correia et al. 2004b; Wersäll et al. 2017; Wersäll et al. 2020), which may have a significant effect on E_{v2} .

Nonlinear soil properties and stress-dependent moduli have significant implications for PLT and its application to railway embankments, which is a well-known fact. Several studies have concluded that the stress level has a significant influence on the deformation modulus during PLT (Dastich and Dawson 1995; Kim and Park 2011), where strain magnitudes may reach 0.1% (Gomes Correia et al. 2004a; Gomes Correia et al. 2004b), thus implying a high degree of nonlinear behavior. Gomes Correia and Cunha (Gomes Correia and Cunha 2014) conducted linear and nonlinear simulations of the response of a ballasted railway track to high-speed railway traffic loading and found that nonlinearity affects stresses and strains down to a depth of approximately 2 m, and that nonlinear modeling is required in order to obtain a sufficient degree of accuracy. Mackiewicz and Krawczyk (Mackiewicz and Krawczyk 2018) concluded that nonlinear models are required to simulate PLT. Li and Baus (Li and Baus 2005) concluded that the stress level in PLT is in the same order of magnitude as the stress applied to the surface of a road and that $E = E_{v2}$ may then be a reasonable assumption. The same cannot be said for slab-track railways, however, where the nonlinear effect is low due to reduced stress magnitude (compared to ballasted tracks) while PLT induces a high degree of nonlinear behavior. Gomes Correia et al. (Gomes Correia et al. 2004a) concluded that if moduli applied in practice are not defined for the relevant stress and strain magnitude, they must be

associated with correction factors. A correction factor of $E = 3.3 \cdot E_{v2}$ has been proposed (Ramos et al. 2021; Ramos et al. 2022).

Young's modulus in frictional soils is also influenced significantly by parameters such as fines content, dry density, and moisture content. The moisture content is especially influential (Li and Baus 2005; Dawson and Gomes Correia 1989; Fortunato et al. 2010). Another important property is the particle size distribution (Andréasson 1973; Mollahasani et al. 2011). In addition, Poisson's ratio is affected by stress and strain, which has been shown by many authors, as discussed in (Park and Lytton 2004). However, the influence of Poisson's ratio on stiffness characteristics is small and this aspect is judged to be of minor influence for E_{v2} evaluation. Additionally, the type of counterweight (e.g., truck, excavator) has been shown to affect PLT results (Mackiewicz and Krawczyk 2018).

In this study, PLTs and railway embankments with ballastless tracks were simulated by finite element (FE) models in PLAXIS 2D with the nonlinear Hardening Soil Model (HSM). Results from four PLTs, conducted on rock-fill embankments in the field, were used to calibrate four FE models of PLT. The obtained soil properties were applied to four corresponding embankment models, which were analyzed in terms of stiffness. Based on the results of the FE modeling, a simple semi-empirical method for estimation of E -modulus based on E_{v2} , obtained through field PLT, is proposed. The method provides, for the first time, the possibility to evaluate PLTs, taking the effect of confinement stress into account, without the use of advanced FE simulations. It can be used to analyze deformation of railway embankments, such as track deflection. Although it is an approximation, the proposed approach provides more realistic results than the conventional assumption of a constant modulus equal to E_{v2} , with or without correction factors.

2 Methodology

FE simulations were conducted in PLAXIS 2D with the HSM, which was proposed by (Schanz et al. 2019) and is based on a hyperbolic stress–strain relationship according to (Duncan and Chang 1970). The HSM has been previously applied successfully to simulate PLTs (Gomes Correia et al. 2004b). Four PLTs on compacted embankments of 0–150-mm crushed rock-fill sub-ballast and varying embankment heights were used as bases for FE simulations of PLT and railway embankments with the purpose of correlating E_{v2} to relevant E -moduli for embankments. The field tests were conducted at various locations on railway embankments with particle size grading according to Swedish regulations for sub-ballast, as shown in Fig. 2. Two geometrical models were built—one for a PLT and one for a ballastless railway embankment. For each of the four PLTs, the following procedure was applied:

1. Simulation of PLT with assumed soil properties.
2. Comparison of the obtained simulated stress-deformation relationship with that measured in the field.
3. Adjustment of assumed soil properties and reiteration of the FE simulation.

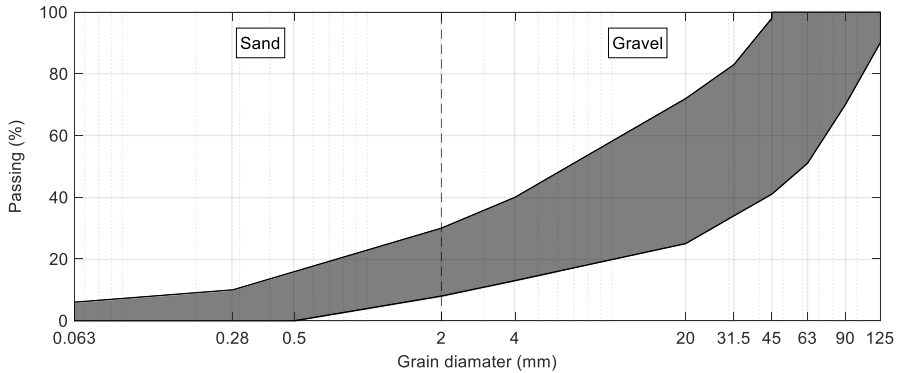


Fig. 2 Minimum and maximum particle size grading according to Swedish regulations for sub-ballast

4. Repetition of steps 2–3 until the correlation between measured and calculated stress-deformation relationships was acceptable. This was obtained in 15–25 simulations per measured PLT.
5. FE simulation of a railway embankment with the final soil properties obtained in step 4.
6. Analysis of the unloading and reloading modulus in the embankment.

2.1 Simulation of PLT and Calibration

Three results are typically presented from a repetitive PLT: the stiffness in the first loading cycle, E_{v1} ; the stiffness in the second loading cycle, E_{v2} ; and the ratio E_{v2}/E_{v1} . The result of the first loading cycle is somewhat influenced by initialization between the plate and the soil and comes with great uncertainties, especially in very coarse-grained soils. Thus, E_{v1} is, in and of itself, of little practical relevance. The second loading cycle is considered the most representative of embankment behavior and E_{v2} is normally used for compaction control and stiffness requirements. The ratio E_{v2}/E_{v1} is considered a measure of the remaining compaction potential of the soil, where a low value corresponds to low remaining compaction potential and vice versa. It is sometimes used as a complement to E_{v2} but should be interpreted with caution due to the inherent uncertainty of E_{v1} . The results of the four PLTs are summarized in Table 1.

Table 1 Summary of evaluated PLTs

PLT no.	E_{v1} (MPa)	E_{v2} (MPa)	E_{v2}/E_{v1} (–)
PLT1	88.7	179.1	2.02
PLT2	69.6	167.0	2.40
PLT3	46.1	150.5	3.26
PLT4	18.5	67.9	3.67

In FE simulation with the HSM, the reloading cycle is linear and follows the unloading cycle according to an unloading and reloading modulus, E_{ur} , given in Eq. 1.

$$E_{ur} = E_{ur}^{ref} \left(\frac{\sigma'_3 + c'}{p_{ref} + c'} \right)^m \quad (1)$$

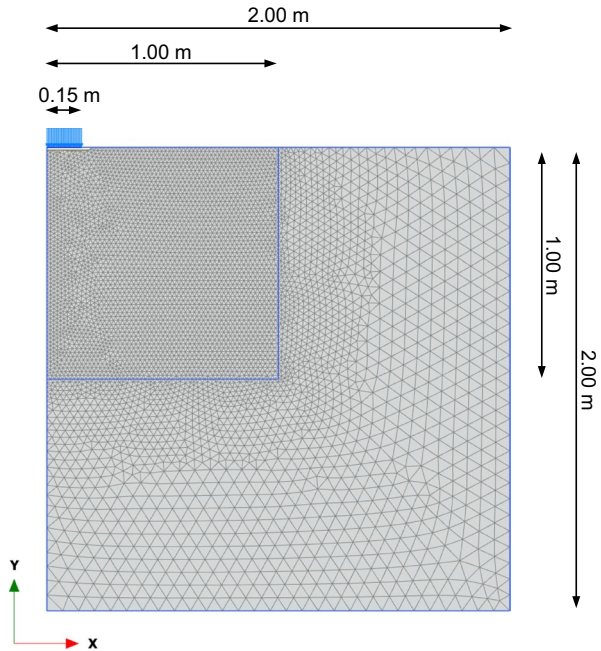
where E_{ur}^{ref} is E_{ur} at the reference stress $\sigma'_3 = p_{ref}$, σ'_3 is the effective minimum principal stress, c' is the effective cohesion, and m is an exponent determining the degree of nonlinearity.

A perfect match for both loading cycles is unobtainable, partly owing to the uncertainty of the first cycle. Another uncertainty of PLT results is the last unloading stage of the first cycle (from the normal stress $\sigma = 120 \text{ kPa}$ to $\sigma = 0$) and the first loading stage of the second cycle (from $\sigma = 0$ to $\sigma = 80 \text{ kPa}$). When reloading over-consolidated soil, the stress–strain relationship should express a practically linear behavior, which corresponds to the unloading behavior (Janbu 1963; Duncan and Bursey 2013). In the last unloading stage and the first reloading stage of PLTs, however, the deformation often suggests a lower stiffness than in subsequent loading stages. This may be attributed to the fact that unloading in PLT is preceded until reaching a fully stressless state, thus requiring re-initialization between plate and soil. Due to the uncertainty of the first cycle and the discrepancy between the second cycle and the expected soil response, the following methodology was adopted for calibrating the FE model to the measured response:

1. The last unloading stage and the first loading stage in the second cycle ($\sigma: 120 \text{ kPa} \rightarrow 0 \rightarrow 80 \text{ kPa}$) were excluded.
2. For the remaining loading stages in the second cycle, a representative unloading and reloading behavior was determined through linear regression of both unloading and reloading combined.
3. Correlation between the unloading cycle in the FE model and the linear regression of the second cycle was prioritized over correlation with the first loading cycle.
4. The iteration was considered acceptable when the simulated behavior matched the final deformation of the first loading cycle and the slope of the linear regression, obtained from the second loading cycle.

PLTs were simulated in PLAXIS 2D HSM through an axisymmetric model with a radius of 2 m and a depth of 2 m, shown in Fig. 3. The soil consisted of one material with properties obtained from the iterative procedure and corresponding to the sub-ballast. Since the sub-ballast thickness is always greater than the influence depth of a PLT (two plate diameters), the soil behaves as an infinite half-space. The mesh was generated in two zones, where the inner zone (closest to the loading plate) had a coarseness factor of 0.1 and the outer zone had a coarseness factor of 0.4. The elements were 15-noded triangular elements. The loading plate was stiff and had a radius of 0.15 m, which corresponds to standardized equipment. The following loading phases were applied:

Fig. 3 Axisymmetric FE model for PLT



1. Initial stresses (K_0 method)
2. Loading (activate the load)
3. Unloading (deactivate the load)

Since no triaxial or other tests, except for PLTs, had been conducted on the rock-fill, all soil properties were initially assumed. These assumptions were adjusted until the calculated response was sufficiently similar to the measured response. Since all four evaluated PLTs were conducted on compacted rock-fill sub-ballast with a particle size range of 0–150 mm, some parameters, presented in Table 2, were assumed constant in all simulations. The parameters that were varied until the results of the model correlated with the measured results are shown in Table 3.

2.2 Simulation of Embankment

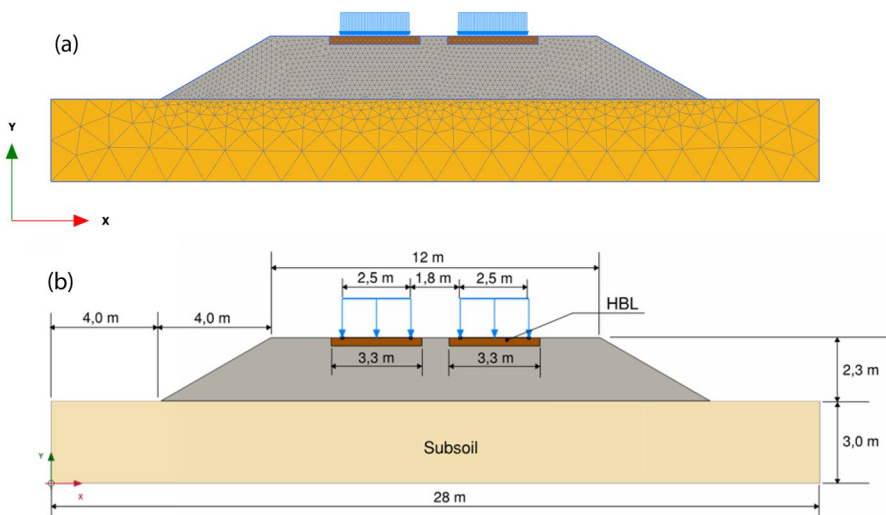
For each of the tests PLT1-4, and their corresponding FE models, a railway embankment was simulated, denoted E1-4, respectively. The embankment was modeled in plane strain with 15-noded triangular elements, shown in Fig. 4a. The dimensions of the embankment are shown in Fig. 4b. The height of the embankment was 2.3 m on a stiff subsoil. The slab tracks were modeled as distributed loads of 33 kPa and widths of 2.5 m with simultaneous loading on both tracks. The loading properties were assumed based on expected characteristics of the planned Swedish high-speed railway lines. Loading was conducted in two cycles with the evaluated results based on the unloading and reloading properties. The following modeling phases were applied:

Table 2 Parameters assumed constant throughout all simulations

Parameter	Denotation in PLAXIS	Value	Comment
Unsaturated unit weight	γ_{unsat}	20 kN/m ³	Unsaturated material was assumed
Cohesion	c'	1.6 kN/m ²	$c' > 0$ must be applied to avoid numerical issues where $\sigma = 0$
Friction angle	ϕ'	45°	Characteristic value from Swedish requirements
Dilation angle	ψ	15°	Calculated by $\psi = \phi' - 30^\circ$
Earth pressure coefficient at rest, OC	$K_{0,r}, K_{0,z}$	0.26	For over-consolidated soil
Reference stress	P_{ref}	100 kPa	Standard value
Reduction factor for failure stress	R_f	0.9	Standard value

Table 3 Varied parameters

Parameter	Denotation in PLAXIS	Comment
Reference modulus	E_{50}^{ref}	Reference for secant modulus at 50% of the failure stress
Reference modulus	E_{oed}^{ref}	Reference for odometer modulus
Reference modulus	E_{ur}^{ref}	Reference for unloading and reloading modulus. See Eq. 1
Exponent	m	Determines the degree of nonlinearity
Poisson's ratio	ν'_{ur}	
Earth pressure coefficient at rest, NC	K_0^{nc}	For normally consolidated soil
Over-consolidation ratio	OCR	The embankment is over-consolidated due to compaction

**Fig. 4** Plane strain FE model of embankment (a) and embankment dimensions (b)

1. Initial stresses in subsoil (K_0 method)
2. Activate railway embankment and HBL
3. Loading (activate the distributed load)
4. Unloading (deactivate the distributed load)

Below each slab was a hydraulic bound layer (HBL) with the width 3.3 m and thickness 0.3 m. Since the stiffness of the HBL was significantly higher than the embankment and its deformation irrelevant for the current application, it was simulated by the Mohr-Coulomb material model. The properties were based on expected characteristics of HBL layers for the planned Swedish high-speed railway network:

unit weight 22 kN/m^3 , Young’s modulus 1 MPa , and Poisson’s ratio 0.3 . The subsoil was modeled as linear elastic with a unit weight of 20 kN/m^3 , Young’s modulus 20 GPa , and Poisson’s ratio 0.3 . The high stiffness of the subsoil was equivalent to a piled slab with end-bearing piles. Since the elastic deformation of piles only affects the total displacement in the superstructure, and not the deformation properties within the embankment, this simplification did not have any effect on the analysis of the embankment material. The embankment was assumed to consist only of crushed rock-fill sub-ballast, modeled in the HSM with properties according to Tables 2 and 3 (results from PLT simulation). The mesh had coarseness factors of 0.1 in the HBL, 0.2 in the embankment, and 0.8 in the subsoil.

3 Results and Discussion

3.1 Plate Load Tests

Figure 5 shows, for each of the four cases PLT1-4, the results from the PLT, the regression of unloading/reloading, and the final FE simulation of the PLT. A perfect match between FE simulations and the first loading cycle was not realistic, as discussed above. The main goals of the iterative simulation procedure were:

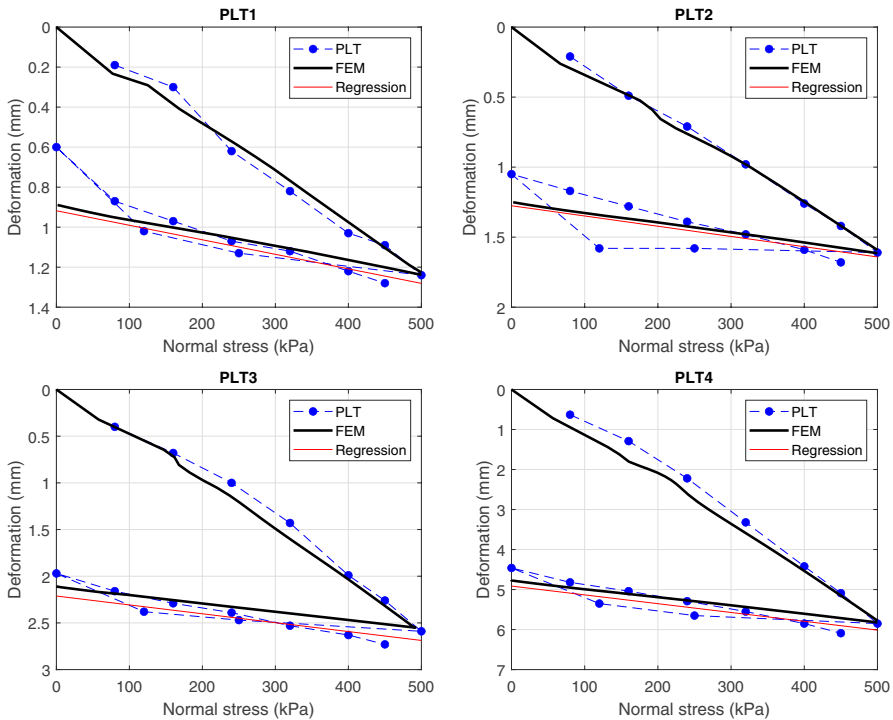


Fig. 5 Results from PLT, linear regression of measured unloading, and reloading behavior and deformation in final FE simulation for each case

1. To match the final measured deformation of the first loading cycle.
2. To match the slope of the regression of the measured unloading and reloading behavior.

After 15–25 iterations per case, the results in Fig. 5 were obtained. The soil properties in the final simulations for each case are shown in Table 4. The high OCR values are motivated by the compaction-induced over-consolidation in combination with the lack of overburden pressure.

3.2 Embankments

The resulting contact stress below the HBL was 40 kPa below its center and 12 kPa below the edges. The variation of E_{ur} within the four embankments E1-4, with soil properties determined through PLT1-4 (Table 4), is shown in Fig. 6. Comparing Fig. 6 to Table 1, it is clear that E_{v2} was close to E_{ur} at the unconfined embankment surface. This implies that E_{v2} can be considered to be an estimate of E_{ur} where $\sigma'_3=0$. As depth and thus confinement stress increased, E_{ur} also increased. Maximum E_{ur} values at the bottom of the embankments were between 2.1 and 2.5 times higher than at the surface, highlighting the importance of considering confinement stress. The influence of the HBL gave rise to a slight lateral variation in E_{ur} . The results from the FE-simulations suggest that PLT can be used to obtain an approximation of unconfined E_{ur} , which can be adjusted for confinement stress through the hyperbolic stress–strain relationship according to (Duncan and Chang 1970). This relationship, however, requires several soil properties, which are typically unknown for embankments. Based on the results from this study, these parameters can be assumed for compacted coarse-grained rock-fill, thus providing a semi-empirical method.

3.3 Semi-Empirical Method

To evaluate E_{ur} from E_{v2} , a semi-empirical approach is proposed based on a hyperbolic stress–strain relationship as in HSM and the results from FE simulations. From the observation that $E_{ur}=E_{v2}$ when $\sigma'_3=0$, and by choosing the reference stress

Table 4 Parameters of final PLT and embankment simulations

Parameter	PLT1/E1	PLT2/E2	PLT3/E3	PLT4/E4
E_{50}^{ref}	110 MPa	95 MPa	65 MPa	30 MPa
E_{oed}^{ref}	110 MPa	95 MPa	68 MPa	30 MPa
E_{ur}^{ref}	630 MPa	600 MPa	510 MPa	210 MPa
m	0.31	0.3	0.31	0.28
ν'_{ur}	0.25	0.25	0.25	0.22
K_0^{nc}	0.30	0.31	0.38	0.32
OCR	30	18	16	10

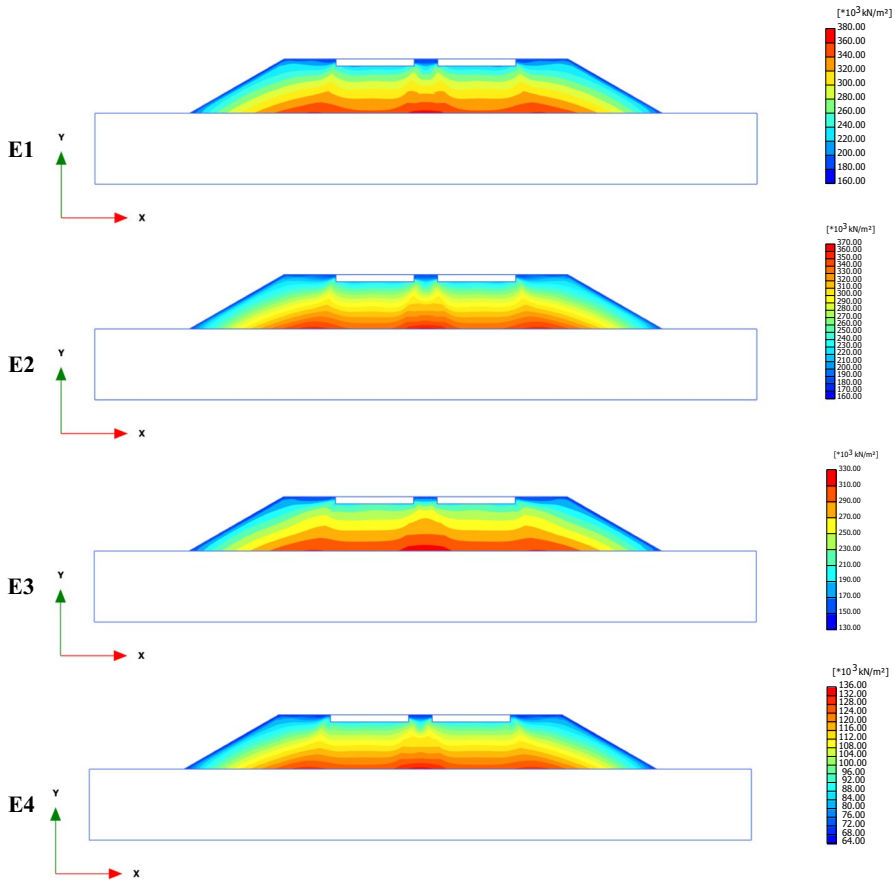


Fig. 6 The variation of E_{ur} within each simulated embankment

$p_{ref}=0$, the reference modulus is given by $E_{ur}^{ref} = E_{v2}$ (cf. Eq. 1). Thus, Eq. 1 simplifies to Eq. 2.

$$E_{ur} = E_{v2} \left(\frac{\sigma'_3 + c'}{c'} \right)^m \tag{2}$$

Assuming that σ'_3 is represented by the horizontal stress, it can be calculated by Eq. 3.

$$\sigma'_3 = K_0 \sigma'_v \tag{3}$$

where K_0 is the at-rest earth pressure coefficient and σ'_v is the effective vertical stress. Note that σ'_v includes the overburden pressure but not the additional traffic load. It is now possible to estimate E_{ur} throughout the embankment by Eq. 2 and by assuming c' , m , and K_0 . In the calibrated FE models presented above, $c' = 1.6 \text{ kPa}$, $m: 0.28 - 0.31$, and $K_0: 0.30 - 0.38$. Based on these results,

the assumptions according to Eqs. 4–6 are proposed for the analyzed material (crushed rock, 0–150 mm). Note that $c' > 0$ must be assumed to avoid numerical problems where $\sigma'_3 = 0$.

$$c' = 1.6 \text{ kPa} \quad (4)$$

$$m = 0.3 \quad (5)$$

$$K_0 = 0.32 \quad (6)$$

By combining Eqs. 2–6, the semi-empirical expression according to Eq. 7 is obtained.

$$E_{ur} = E_{v2} (0.2\sigma'_v + 1)^{0.3} \quad (7)$$

To evaluate the accuracy of the semi-empirical approach in relation to the simulations in PLAXIS HSM, E_{ur} was calculated by Eq. 7 and compared to the FE results. Since the comparison was made with the same data on which the method is based, it is not to be considered a validation. To include the unconfined embankment surface, a section 1.1 m outside the extent of the HBL was chosen. This section also had a very similar modulus variation as below the center of the HBL (see Fig. 6). The assumed unit weight was $\gamma = 20 \text{ kN/m}^3$ (as for the FE model). Figure 7 shows the variation of E_{ur} with depth from the embankment surface, z , estimated by the semi-empirical approach and calculated by the FE model. The accuracy of the simplified method is considered sufficient for many engineering applications.

To validate the semi-empirical approach for settlements during PLTs, the method was compared to 43 other PLTs on crushed rock with particle size grading 0–150 mm and within the boundaries shown in Fig. 2. The PLTs were conducted in various locations. The plate diameter was 300 mm in all tests. From each PLT, the settlement in the second loading cycle was compared to the semi-empirically calculated settlement based on the measured E_{v2} . Settlements were calculated by the following procedure:

1. Divide the soil into layers of 0.01 m from the embankment surface to a depth of 10 m.
2. Calculate the overburden pressure (σ'_v) with the assumption $\gamma = 20 \text{ kN/m}^3$.
3. Calculate E_{ur} by Eq. 7, using the measured E_{v2} .
4. Calculate the distribution of the additional load from the plate by Boussinesq's stress distribution, given in Eq. 8 (below).
5. Calculate the vertical strain in every layer, $\varepsilon = \Delta\sigma_v / E_{ur}$.
6. Multiply the vertical strain by the layer thickness of each layer.
7. Calculate the sum of the settlements in all layers.

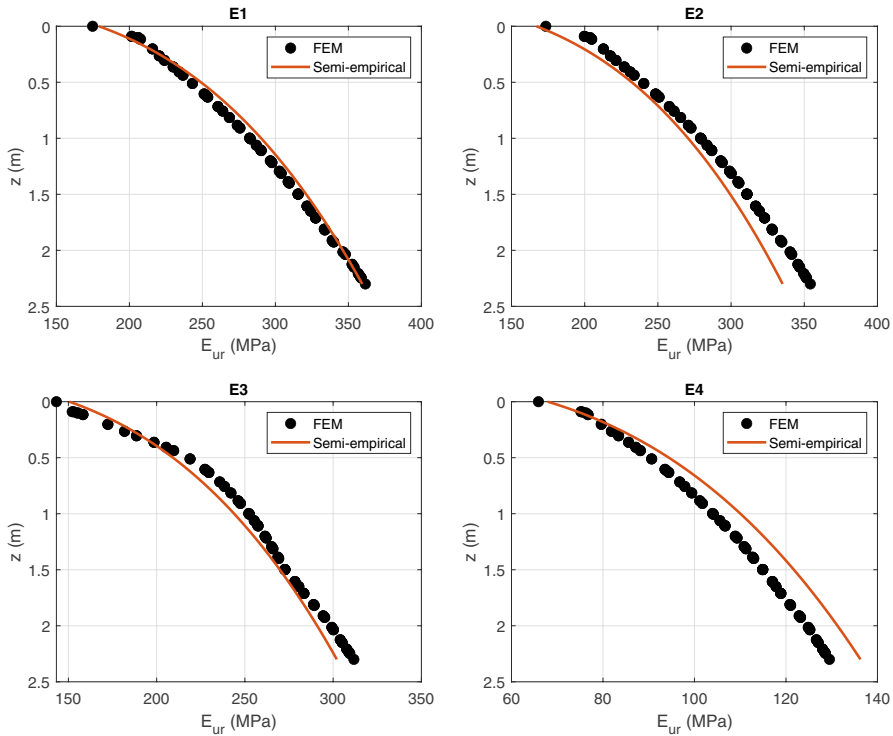


Fig. 7 Semi-empirically calculated E_{ur} compared to results of FE simulations

$$\Delta\sigma_v = q \left(1 - \frac{1}{\left(\left(\frac{R}{z} \right)^2 + 1 \right)^{3/2}} \right) \tag{8}$$

where $q=450 \text{ kPa}$ is the load from the plate at the end of the second loading cycle, $R=0.15 \text{ m}$ is the radius of the plate, and z is the depth from the embankment surface.

Comparisons between the settlements calculated by the above procedure and the measured settlements in the second loading cycle are shown in Fig. 8. For reference, the figure also shows the corresponding settlements calculated by the simplification $E_{ur}=E_{v2}$. The measured settlements and those calculated by the semi-empirical method correlate well, while the assumption $E_{ur}=E_{v2}$ overestimates the settlements.

The difference in calculated settlement by the semi-empirical approach and that based on the assumption $E_{ur}=E_{v2}$ was quite small for the PLTs above. This was expected since the stress conditions of the calculated case matched the test conditions. When the contact area between the foundation and the embankment increases (such as for a railway slab track), the stress and stiffness conditions during PLT and

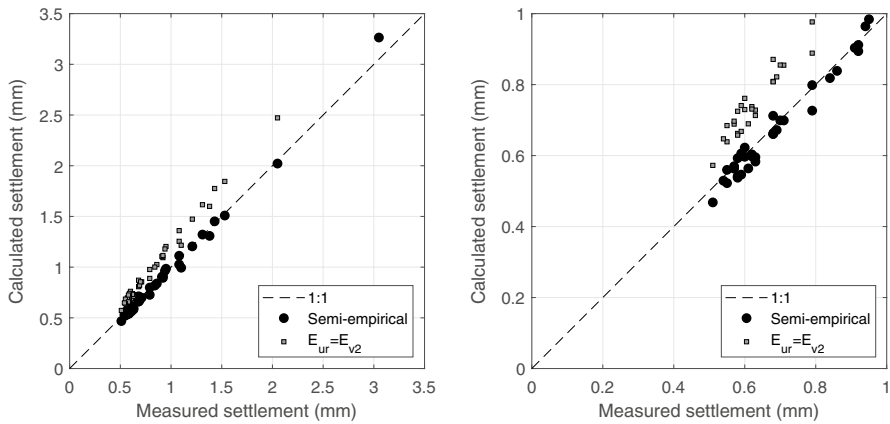


Fig. 8 Measured settlement in the second cycle of 43 PLTs, compared to settlement calculated semi-empirically and by the assumption that $E = E_{v2}$: all values (left) and settlements below 1.0 mm (right)

those during operation become significantly different. In addition, the stress magnitude is considerably different. Thus, using E_{v2} directly as E_{ur} is then more conservative than for calculation of settlement during PLT. To compare the semi-empirical and simplified ($E_{ur} = E_{v2}$) approaches, the settlement of embankment E3 was calculated by both methods. The measured value of E_{v2} was 150.5 MPa in PLT3. Using that value, dividing the embankment into layers, and using Boussinesq's stress distribution in the same manner as described above, the resulting settlement calculated by the semi-empirical method was 0.21 mm. The simplified method of assuming the constant stiffness of $E_{ur} = E_{v2}$ gave 0.35 mm, while the settlement determined by the FEM-model was 0.17 mm. The discrepancy between the FEM-model and the semi-empirical method is mainly attributed to the incapability of Boussinesq's stress distribution to accurately account for distribution through the HBL. Although the semi-empirically calculated settlement was slightly above that determined by the FEM-model, the obtained settlements were fairly similar. The assumption $E_{ur} = E_{v2}$, however, gave more than double the settlement as compared to the FEM-model and is thus considered too conservative. The above results suggest that the semi-empirical method can be an acceptable simplification when determining embankment stiffness for track deflection. Since rail pads determine the majority of track stiffness, the embankment plays a minor role, which is why the assumption $E = E_{v2}$ is often applied in practical engineering situations. This study shows that the proposed semi-empirical approach is a more reliable option, while still offering simplicity. For cases with high accuracy requirements, FE simulation should be applied. It is then necessary to use an advanced soil model, such as HSM, to capture nonlinear behavior. The influence of dynamic train loads was beyond the scope of this study and was not accounted for. Dynamic loads mainly occur due to track irregularities and their effect on the present investigation was considered insignificant for evaluation of embankment stiffness.

4 Conclusions

FE simulations of PLTs were calibrated against field data. The resulting soil properties were used to simulate high-speed railway embankments, which were analyzed in terms of embankment stiffness. The main findings are listed below.

- Young's modulus at the unconfined embankment surface corresponds to the E_{v2} -modulus obtained from a PLT. With increasing depth, and thus confinement stress, the stiffness deviates significantly from E_{v2} .
- In practice, $E = E_{v2}$ is often assumed but was found too conservative since it does not account for confinement stress.
- A semi-empirical method was proposed to account for the influence of confinement stress on Young's modulus through a hyperbolic stress–strain relationship with assumptions of soil properties based on results from FE analyses.
- The study was conducted on compacted rock-fill with particle size grading 0–150 mm, for which assumptions of soil properties for the semi-empirical method were presented and evaluated. The method and assumptions were validated against 43 PLTs on the same type of material, which showed a good agreement.
- The results showed that the accuracy of the semi-empirical method can be considered sufficient for many engineering applications and that it constitutes an improvement compared to conventional analysis techniques. However, for high requirements on accuracy, advanced FE models are recommended.

Acknowledgements The authors thank Ulf Ryberg at Sweco for supplying field data.

Author Contribution CW interpreted the results and wrote the manuscript. SB conducted the FE simulations and analyzed the results. PZ formulated the problem statement and conceptualized the study. All authors read and approved the final manuscript.

Funding Open access funding provided by Royal Institute of Technology. This study was funded by the Swedish Transport Administration (grant number TRV2019/53534).

Availability of Data and Materials The datasets used and analyzed during the current study are available from the corresponding author on reasonable request.

Declarations

Ethics Approval and Consent to Participate Not applicable.

Consent for Publication Not applicable.

Competing Interests The authors declare no competing interests.

Open Access This article is licensed under a Creative Commons Attribution 4.0 International License, which permits use, sharing, adaptation, distribution and reproduction in any medium or format, as long as you give appropriate credit to the original author(s) and the source, provide a link to the Creative

Commons licence, and indicate if changes were made. The images or other third party material in this article are included in the article's Creative Commons licence, unless indicated otherwise in a credit line to the material. If material is not included in the article's Creative Commons licence and your intended use is not permitted by statutory regulation or exceeds the permitted use, you will need to obtain permission directly from the copyright holder. To view a copy of this licence, visit <http://creativecommons.org/licenses/by/4.0/>.

References

- Andréasson, L.: Kompressibilitet hos friktionsjord [Compressibility of frictional soil]. PhD thesis, Chalmers Tekniska Högskola, Göteborg. (1973) (in Swedish).
- Burmister, D.M.: Symposium on load tests of bearing capacity of soils. General Discussion. ASTM STP. **79**, 139–148 (1947)
- Dastich, I., Dawson, A.: Techniques for assessing the nonlinear resilient response of unbound granular-layered structures. *Geotec. Test. J.* **18**(1), 50–57 (1995)
- Dawson, A.R., Gomes Correia, A.: The effects of stress and pore water pressure states on the resilient properties of granular materials. In: 12th International Conference on Soil Mechanics and Foundation Engineering, Rio de Janeiro, Brazil. 1 (1989)
- Deutsches Institut für Normung: Determining the deformation and strength characteristics of soil by plate loading test. DIN 18134, the German Institute for Standardization (2012)
- Duncan, J.M., Bursey, A.: Soil modulus correlations. In: *Foundation Engineering in the Face of Uncertainty: Honoring Fred H. Kulhawy*, Geotechnical Special Publication 229, ASCE. 321–336 (2013)
- Duncan, J.M., Chang, C.Y.: Nonlinear analysis of stress and strain in soils. *J. Soil Mech. Found. Div.* **96**(5), 1629–1653 (1970)
- Elsamee, W.N.A.: An experimental study on the effect of foundation depth, size and shape on subgrade reaction of cohesionless soil. *Engineering*. **5**, 785–795 (2013)
- Fortunato, E., Pinelo, A., Fernandes, M.M.: Characterization of the fouled ballast layer in the substructure of a 19th century railway track under renewal. *Soils. Found.* **50**(1), 55–62 (2010)
- Gomes Correia, A., Cunha, J.: Analysis of nonlinear soil modelling in the subgrade and rail track responses under HST. *Transp. Geotech.* **1**(4), 147–156 (2014)
- Gomes Correia, A., Viana da Fonseca, A., Gambin, M.: Routine and advanced analysis of mechanical in situ tests: results on saprolitic soils from granites more or less mixed in Portugal. In: *Second International Conference on Site Characterization*, Porto, Portugal. 2, 75–95 (2004a)
- Gomes Correia, A., Antão, A., Gambin, M.: Using non linear constitutive law to compare Menard PMT and PLT E-moduli. In: *Proceedings of the 2nd International Conference on Site Characterization*, Porto, Portugal. 927–933 (2004b)
- Janbu, N.: Soil compressibility as determined by odometer and triaxial tests. In: *Proceedings of European Conference on Soil Mechanics and Foundation Engineering*, Weisbaden, Germany. 1, 19–25 (1963)
- Kim, D., Park, S.: Relationship between the subgrade reaction modulus and the strain modulus obtained using a plate loading test. In: *9th World Congress on Railway Research*, Lille, France (2011)
- Li, T., Baus, R.L.: Nonlinear parameters for granular base materials from plate tests. *J. Geotec. Geoenviron.* **131**(7), 907–913 (2005)
- Mackiewicz, P., Krawczyk, B.: Influence of the load and time conditions on the results of the static plate load test. *J. Test. Eval.* **48**(4), 2963–2980 (2018)
- Mollahasani, A., Alavi, A.H., Gandomi, A.H.: Empirical modeling of plate load test moduli of soil via gene expression programming. *Comput. Geotech.* **38**(2), 281–286 (2011)
- Park, S.W., Lytton, R.L.: Effect of stress-dependent modulus and Poisson's ratio on structural responses in thin asphalt pavements. *J. Transp. Eng.* **130**(3), 387–394 (2004)
- Ping, W.V., Ge, L.: Field verification of laboratory resilient modulus measurements on subgrade soils. *Transportation Res. Rec.* **1557**, 53–61 (1997)
- Ramos, A., Gomes Correia, A., Calçada, R., Alves Costa, P., Esen, A., Woodward, P.K., et al.: Influence of track foundation on the performance of ballast and concrete slab tracks under cyclic loading: physical modelling and numerical model calibration. *Constr. Build. Mater.* **277**, 122245 (2021)
- Ramos, A., Gomes Correia, A., Calçada, R., Connolly, D.P.: Ballastless railway track transition zones: an embankment to tunnel analysis. *Transp. Geotech.* **33**, 100728 (2022)
- Schanz, T., Vermeer, P.A., Bonnier, P.G.: The hardening soil model: formulation and verification. In: *Beyond 2000 in Computational Geotechnics*, Routledge. 281–296 (2019)

- Trafikverket: Bestämning av bärighetsegenskaper med statisk plattbelastning [Determination of bearing properties by static plate loading]. TDOK 2014:0141, the Swedish Transport Administration (2014) (in Swedish)
- Wersäll, C., Nordfelt, I., Larsson, S.: Soil compaction by vibratory roller with variable frequency. *Géotechnique*. **67**(3), 272–278 (2017)
- Wersäll, C., Nordfelt, I., Larsson, S.: Roller compaction of rock-fill with automatic frequency control. *P. I. Civil Eng.-Geotech.* **173**(4), 339–347 (2020)

Publisher's Note Springer Nature remains neutral with regard to jurisdictional claims in published maps and institutional affiliations.